MOLECULAR PLANT PATHOLOGY (2005) **6**(2), 165–176 DOI: 10.1111/J.1364-3703.2005.00275.X

An atypical 3′-controller element mediates low-level transcription of the p6 subgenomic mRNA of *Citrus tristeza virus*

MARÍA A. AYLLÓN†, TATINENI SATYANARAYANA, SIDDARAME GOWDA AND WILLIAM O. DAWSON*

Department of Plant Pathology, University of Florida, Citrus Research and Education Center, Lake Alfred, FL 33850, USA

SUMMARY

Citrus tristeza virus (CTV) has within the 3′-half of the genome ten open reading frames (ORFs) that are expressed through a series of 3′-coterminal subgenomic (sg) messenger (m)RNAs that, in general, function as monocistronic mRNAs with only the 5′-most ORF translated. Yet only nine sg mRNAs have been detected, suggesting that ORF 3, which is predicted to encode a small hydrophobic protein of ~6 kDa (p6), might be expressed in some other manner, perhaps from a functionally dicistronic sg mRNA. However, when we positioned the p6 gene near the 3′-terminus of a minimal CTV replicon to amplify greatly the level of production of the putative sg mRNA, we found a minimal level of a p6 mRNA, thus providing evidence for a separate mRNA for each 3′ ORF. The 5′ termini of the sg mRNAs and the *cis*-acting elements (controller elements—CEs) that regulate the production of the p6 gene and the adjacent HSP70h (heat shock protein 70 homologue) were located further upstream of the ORFs compared with the other CTV CEs. Both preferentially initiated synthesis with an adenylate, as has been shown for the more highly expressed 3′ genes; but in contrast, the p6 sg mRNA occasionally initiated with a guanylate. Although the nucleotide sequences and the computer-predicted secondary structures of the HSP70h CE were similar to those previously described for other 3′ CEs, those of the p6 CE were quite different, suggesting that CE strength is related to proximity to an ideal CE conformation. The lack of similarity between different CTV CEs led us to examine how well the CTV replicase complex could initiate sg mRNAs from CEs from different members of the family *Closteroviridae*. We found that the CTV replicase complex efficiently initiated production of sgRNAs from the p6 and HSP70h CEs from *Beet yellows virus*, with the HSP70h CE initiating at the same nucleotide as within the homologous virus, indicating that the mode of recognition of the CEs is similar. However, CEs from a more distantly related member of the *Closteroviridae*, *Lettuce infectious yellows virus*, did not function to produce sg mRNAs in CTV.

* *Correspondence*: Tel.: +1 863 956 4311 ext. 1361; Fax: +1 863 956 4631; e-mail: wodtmv@crec.ifas.ufl.edu

† *Present address*: Departamento de Biotecnología, E.T.S.I. Agrónomos, Universidad Politécnica de Madrid, 28040, Spain.

INTRODUCTION

The family *Closteroviridae* comprises genera with monopartite genomes, *Closterovirus* and *Ampelovirus*, and with bipartite or tripartite genomes, *Crinivirus*. *Citrus tristeza virus* (CTV), a *Closterovirus*, is one of the more complex plant viruses, with a positive-stranded RNA genome of ~20 kb organized into 12 open reading frames (ORFs) (Karasev *et al.*, 1995; Pappu *et al.*, 1994). ORFs 1a and 1b are expressed from the genomic RNA by polyprotein processing and ribosomal frameshifting. ORFs 2–11, which make up the 3′ half of the genome, are expressed via 3′-coterminal subgenomic (sg) messenger (m)RNAs (Hilf *et al.*, 1995) that are produced by an undefined mechanism. Two disparate mechanisms for production of sg mRNAs have been established for other positive-stranded RNA viruses: (1) internal promotion with initiation of the positive-stranded sgRNA at a specific *cis*-acting sequence or structure on the genomic negative strand and termination at the 5′-terminus of the genomic complement; and (2) amplification of the positive-stranded sg mRNAs from an sg minus-stranded template, which first is produced by initiation at the 3′-terminus of the genomic RNA and termination at a specific internal site (van Marle *et al.*, 1999; Miller and Koev, 2000; Sawicki and Sawicki, 1998; White, 2002). Because a promotion or termination mechanism for the production of CTV sg mRNAs has not been established, we refer to the *cis*-acting elements that regulate the production of sg mRNAs as controller elements (CEs).

We have characterized the CEs of the six 3′-most genes, which are more highly expressed (Ayllón *et al.*, 2003, 2004; Gowda *et al.*, 2001). In general, the CEs are located upstream of the corresponding ORF with predicted stem-loop structures. Using the positive-sense sequence as a reference, an initiation site, which corresponds to the 5′-terminal nucleotide (nt) of the positive-stranded sgRNA, occurs at the base of the stem near the 3′ border of the minimal CE. The preferred nucleotide for initiation of the

3′-coterminal sg mRNAs is an adenylate (Ayllón *et al.*, 2003; Karasev *et al.*, 1997). A complication is that each CE controls, in addition to the sg mRNA, the production of two other sgRNAs (Gowda *et al.*, 2001). One is a negative-stranded sgRNA complementary to the mRNA, the production of which is modulated by the viral p23 gene product (Satyanarayana *et al.*, 2002b). Deletion of the p23 gene results in large increases in sg minus strands without a corresponding increase in sg plus strands. The second additional RNA species is a positive-stranded sgRNA corresponding to the genomic sequence beginning at the 5′-terminus and terminating within the CE and appears to be produced by premature termination at the CE region during positive-stranded RNA synthesis (Ayllón *et al.*, 2003).

CTV has a different type of CE near the 5′ end of the genome that produces a large amount of a population of 5′-coterminal positive-stranded sgRNA of approximately 700 nt, and a minimal amount of a 3′-terminal positive-stranded sgRNA that initiates within the 5′ CE. This 3′-terminal sgRNA appears to be produced by promotion (internal initiation) because, in contrast to the sg messengers of the 3′ genes, there is no corresponding complementary sg negative strand (Gowda *et al.*, 2001, 2003).

The expression of ten different genes by sg mRNAs from a single RNA molecule, including regulation of timing (Navas-Castillo *et al.*, 1997) and the levels of accumulation of the different sg mRNAs, which differ by probably more than 1000-fold (Hilf *et al.*, 1995), would appear to be a substantial challenge for a virus. What factors influence the levels of production of any specific sg mRNA? Based on the organization of the genome, CTV has two types of 3′ CEs: those located in non-translated regions (NTRs) that occur between ORFs, perhaps with the sole function of controlling expression of the gene; and more restricted CEs located within an upstream ORF. In general, those located within NTRs effect higher levels of sgRNA production. The existence of a virus with many different CEs that are recognized, perhaps differentially, by the same replicase complex would appear to offer a unique opportunity to study *cis*-acting elements regulating sgRNA production.

Because a different sg mRNA appears to be made for each of the 3′ genes, they are thought to be functionally monocistronic with only the 5′-most ORF translated, even though technically they are polycistronic (except for the 3′-most gene). Yet we have been able to detect only nine sg mRNAs for the ten 3′ genes. ORF 3 is small, predicted to encode a hydrophobic protein of ~6 kDa (p6) (Karasev *et al.*, 1994). Deletions within the p6 ORF of CTV or the related *Closterovirus*, *Beet yellows virus* (BYV), result in mutants able to replicate and assemble into virions, but unable to infect plants, suggesting that the p6 ORF is expressed as a movement-related protein (Alzhanova *et al.*, 2000; T.S., unpublished data). In addition, the BYV p6 has been shown to be associated with rough endoplasmic recticulum in infected cells (Peremyslov *et al.*, 2004). Our lack of ability to detect the tenth sg mRNA led us to wonder whether the p6 gene has a dedicated mRNA produced at levels below our detection, or whether it is translated from a functionally dicistronic messenger, along with either the p33 or the HSP70h gene. The recent demonstration that the BYV p6 is expressed from its own sg mRNA (Peremyslov and Dolja, 2002) suggests that CTV might also produce a dedicated p6 mRNA at minimal levels.

Here we report that CTV does produce a separate sg mRNA for the p6 ORF, but at extraordinarily low levels, barely detectable even when maximally amplified by moving the CE near the 3′-terminus of a replicon. This observation provided an opportunity to compare the extremely weak CE of p6 with the adjacent and potentially stronger CE of HSP70h and to the other 3′ CEs that have been characterized. This comparison was made by mapping the size and location of the minimal active *cis*-acting elements and identifying the initiation nucleotides for the production of the sg mRNAs. Both the p6 and the HSP70h CEs mapped further upstream of their respective ORFs than those of the other 3′ CEs. The predicted secondary structure and the sg mRNA initiation site of the HSP70h CE were similar to those of previously characterized CEs, but those of the p6 CE were not. These results suggest that similarity to an optimum structure is one determinant of the level of activity of the CE. We then examined the ability of the CTV replicase complex to recognize other divergent sg mRNA CEs from other members of the *Closteroviridae*. Both p6 and HSP70h CEs of BYV functioned in CTV, with the BYV p6 CE producing even more sg mRNA than the homologous CTV p6 CE. However, those of the divergent *Lettuce infectious yellows virus* (LIYV) did not effect sgRNA production in CTV.

RESULTS

Identification of two sg mRNAs for the p6 and HSP70h genes

One question was: is there a dedicated sg mRNA for the p6 gene? Examining the production of a specific sgRNA is difficult using the full-length virus with nine visible sgRNAs because the larger sg mRNAs, which tend to be made in lower amounts, are poorly resolved by agarose gel electorphoresis. Deletions to define CEs make the discrimination of different sg mRNAs even more difficult. However, we previously found that positioning poorly expressed genes near the 3′ terminus of smaller replicons greatly increased their levels of sgRNA, and production of one or two small truncated sg mRNAs simplified detection (Satyanarayana *et al.*, 1999). Figure 1(E) shows the differences in production of sgRNAs from the p33 CE when moved from its native position (Fig. 1A) to near the 3′ end of the genome (Fig. 1B). Thus, to identify CEs that produce sg mRNAs to express the p6 and/or HSP70h ORFs, we created a series of constructs containing sequences upstream and including the 5′ portions of the p6 and HSP70h ORFs inserted near the 3′ end of the replicon CTV-ΔCla333 (Fig. 1C;

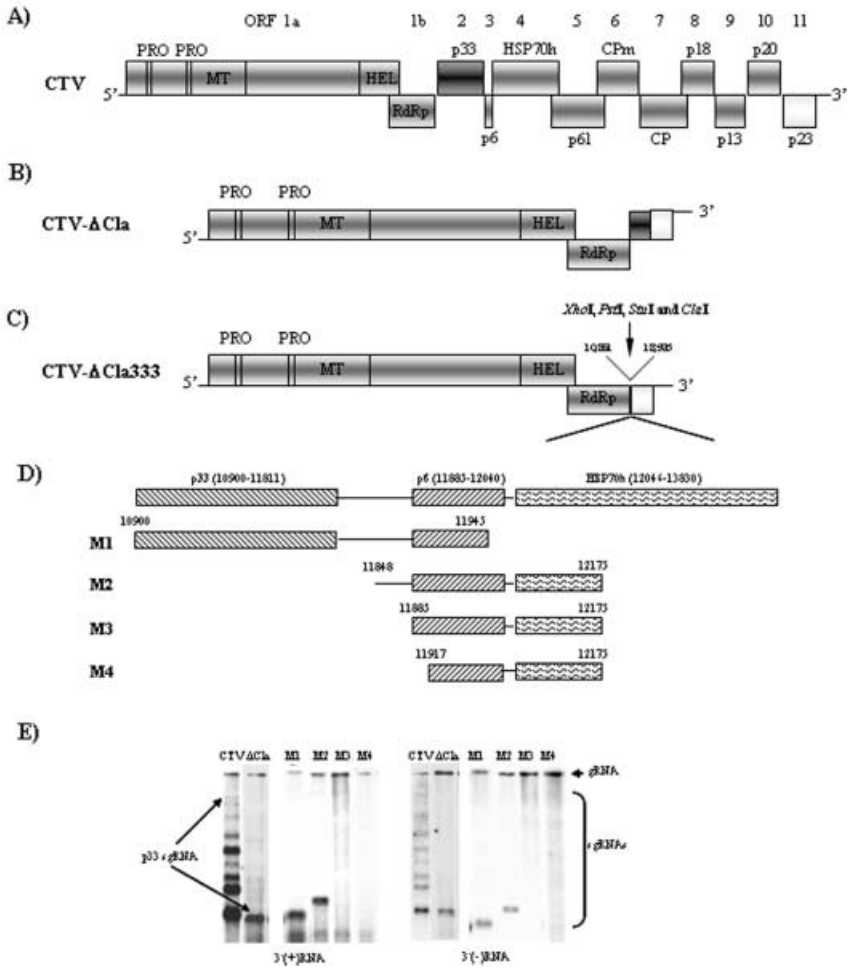

Fig. 1 Location of the HSP70h sgRNA controller element. (A) Schematic diagram of the CTV genome. Boxes represent the ORFs with the respective numbers and encoded products (PRO, protease-like domain; MT, methyltransferase-like domain; HEL, helicase-like domain; RdRp, RNA-dependent RNA polymerase-like domain; HSP70h, homologue of HSP70; CPm, minor coat protein; CP, major coat protein). Schematic diagram of the replicon CTV-ΔCla (B) created by deletion of nucleotides 11011–18525 of CTV and the replicon CTV-ΔCla333 (C) created by deletion of nucleotides 10852–18525. Restriction sites (*Xho*I, *Pst*I, *Stu*I, *Cla*I) were inserted between nucleotides 10851 and 18526. (D) Genomic regions inserted in CTV-ΔCla333. Hatched areas represent p33, p6 and HSP70h ORFs with the numbers in parentheses indicating the positions of the first and last nucleotide of the start and stop codons, respectively. Other numbers represent the 5′ and 3′ boundaries of the regions inserted in CTV-ΔCla333 for mutants M1–M4. (E) Northern blot hybridization analysis of total RNA isolated 4 dpi from *N. benthamiana* mesophyll protoplasts inoculated with *in vitro*-produced RNA transcripts. The blots were hybridized with 3′-terminal positive- or negative-stranded, RNA-specific digoxigenin-labelled RNA probes of 900 nt. The positions of the genomic RNA (gRNA) and the 3′-terminal sg mRNAs are indicated by an arrow and a bracket, respectively. The p33 sgRNA produced from the full-length virus (CTV) and CTV-ΔCla are indicated by long arrows.

Gowda *et al.*, 2001), which has all of the 3′ ORFs and CEs deleted such that no sgRNA is produced from the replicon. Four different regions were cloned in CTV-ΔCla333 to produce mutants M1 to M4 (Table 1; Fig. 1D). M1 contained the p33 ORF without its CE, the NTR (73 nt) between the p33 and p6 ORFs, and the first 61 nt of the p6 ORF. M2 contained part of the p33-p6 NTR, the p6 ORF, the 5 nt NTR between the p6 and HSP70h ORFs, and the first 130 nt of the HSP70h ORF. Mutant M3 differed from M2 by deletion of the p33-p6 NTR, and M4 differed by additional deletion of the 5′ portion of the p6 ORF.

In vitro produced RNA transcripts of these mutants were used to inoculate *Nicotiana benthamiana* mesophyll protoplasts, and total RNA was extracted from protoplasts harvested at 4 days post-inoculation (dpi). The accumulation of sg mRNAs was analysed by Northern blot hybridizations using probes specific to positive- or negative-stranded RNAs corresponding to the 3′ end of the CTV genome. All mutants replicated in protoplasts and produced positive- and negative-stranded genomic RNAs, but only M1 and M2 produced sg mRNAs—both positive- and negative-stranded 3′-terminal sgRNAs (Fig. 1E). However, both M1 and M2 produced only one visible positive-stranded sgRNA species. The sizes of these sg mRNAs were approximately proportional to the sizes of the inserts plus the 3′ end of the replicons, suggesting that only one sg mRNA was produced for the two ORFs, or that a second sg mRNA was produced at a level too low to be detected, or that two sg mRNAs were of sizes too similar to be distinguished.

Previously, we showed that the 5′ and 3′ (273 nt) NTRs, plus ORFs 1a and 1b, were sufficient for optimal replication of CTV (Satyanarayana *et al.*, 1999, 2002a). We generated two sets of mutants, one containing 446 nt of the 3′ end (mutants M6 and M8) and the other containing only the last 280 nt (mutants M5 and M7) (Fig. 2B). Mutants M7 and M8 had the previously examined area (nucleotides 11658–11935) inserted, whereas mutants M5 and M6 had a smaller insertion designed to omit the previously located CE (nucleotides 11848–11945). Two sg mRNAs were observed from mutants M7 and M8, corresponding to the p6 and HSP70h genes (Fig. 2B). M5 and M6 produced minimal amounts of only a single sgRNA, corresponding to the truncated p6 sgRNA. The putative p6 sgRNA accumulated in higher amounts when

Table 1 Mutants and their parent plasmid used in this study.

Mutant	Description of mutation and nt coordinates (5′–3′) of positive (+) and negative (–) primers
pCTV-ΔCla333	parent plasmid, replicon with no sgRNA (Gowda *et al.*, 2001) (Fig. 1). Deletion between nt 10852–18525
M1	nt 10900–11945 (C479(+) nt 10900–10922/C204(–) nt 11945–11921)
M2	nt 11848–12175 (C857(+) nt 11848–11867/C253(–) nt 12175–12141)
M3	nt 11885–12175 (C856(+) nt 11885–11904/C253)
M4	nt 11917–12175 (C600(+) nt 11917–11944/C253)
M5	nt 11658–11857 (nt 11858–19013 deleted) (C579(+) nt 11658–11684/C1282(–) nt 11857–11832; C1281(+) nt 19014–19035/C57(–) nt 19293–19274)
M6	nt 11658–11857 (C579/C1280(–) nt 11857–11832)
M7	nt 11658–11935 (nt 11936–013 deleted) (C579/C1286(–) nt 11935–11917; C1285(+) nt 19014–19033/C57)
M8	nt 11658–11935 (C579/C1284(–) nt 11935–11917)
M9	BYV nt 9212–9422 (C1291(+) nt 9212–9237/C1288(–) nt 9422–9398)
M10	BYV nt 9212–9520 (C1291/C1290(–) nt 9520–9497)
M11	nt 11658–11945 (C579/C204)
M12	nt 11658–11905 (C579/C889(–) nt 11905–11878)
M13	nt 11658–11887 (C579/C891(–) nt 11887–11863)
M14	nt 11658–11884 (C579/C890(–) nt 11884–11858)
M15	nt 11658–11867 (C579/C892(–) nt 11867–11842)
M16	nt 11812–11945 (C887(+) nt 11812–11833/C204)
M17	nt 11848–11945 (C857/C204)
M18	nt 11858–11945 (C956(+) nt 11858–11880/C204)
M19	nt 11868–11945 (C888(+) nt 11868–11888/C204)
M20	nt 11885–11945 (C856/C204)
M21	nt 11848–11905 (58 nt) (Template M12) (C857/C57)
M22	nt 11858–11905 (48 nt) (Template M12) (C956/C57)
M23	nt 11848–11887 (40 nt) (Template M13) (C857/C57)
M24	nt 11858–11887 (30 nt) (Template M13) (C956/C57)
M25	nt 10900–12175 (nt 11858–11884 deleted) (C479/C886(–) nt 11857–11832; C885(+) nt 11885–11905/C253)
M26	nt 11668–11857 (C1497(+) nt 11668–11691/C57)
M27	nt 11714–11857 (C1411(+) nt 11714–11731/C57)
M28	nt 11753–11857 (C1412(+) nt 11753–11770/C57)
M29	nt 11779–11857 (C1413(+) nt 11779–11796/C57)
M30	nt 11812–11857 (C887/C57)
M31	nt 11658–11766 (C579/C1433(–) nt 11766–11745)
M32	nt 11658–11730 (C579/C1434(–) nt 11730–11711)
M33	nt 11658–11711 (C579/C1465(–) nt11711–11689)
M35	compensatory changes in M34
M36	site-specific changes in predicted secondary structure of p6 CE in M6
M37	compensatory changes in M36

expressed alone. The accumulation of the putative p6 sgRNA appeared to be reduced by competition with the other CE. The production of sg mRNAs from mutants M5 and M6 indicated that the p6 CE was located in the region between nucleotides 11658 and 11857, whereas the results obtained from mutants M2, M7 and M8 indicated that HSP70h CE was located between nucleotides 11848 and 11935 (Figs 1E and 2B).

Mapping the HSP70h CE

To delineate the HSP70h CE, we created a series of deletions at each side of the previously identified region to define a minimal element. To map the 3′ boundary, a series of fragments with a constant 5′-terminus at nucleotide 11658 and 3′ termini at nucleotides 11945, 11905, 11887, 11884 or 11867 were ligated into CTV-ΔCla333 (mutants M11–M15, respectively; Fig. 3A). All five mutants replicated efficiently, producing positive- and negative-stranded genomic RNAs; however, only mutants M11–M13 accumulated sg mRNAs (Fig. 3B), suggesting that the 3′ boundary of the HSP70h CE mapped between nucleotides 11887 and 11884, near the start codon of the p6 ORF.

To delineate the 5′ boundary of the HSP70h CE, we created mutants M16–M20 with a constant 3′ end at nucleotide 11945 and 5′-termini at nucleotides 11812, 11848, 11858, 11868 or

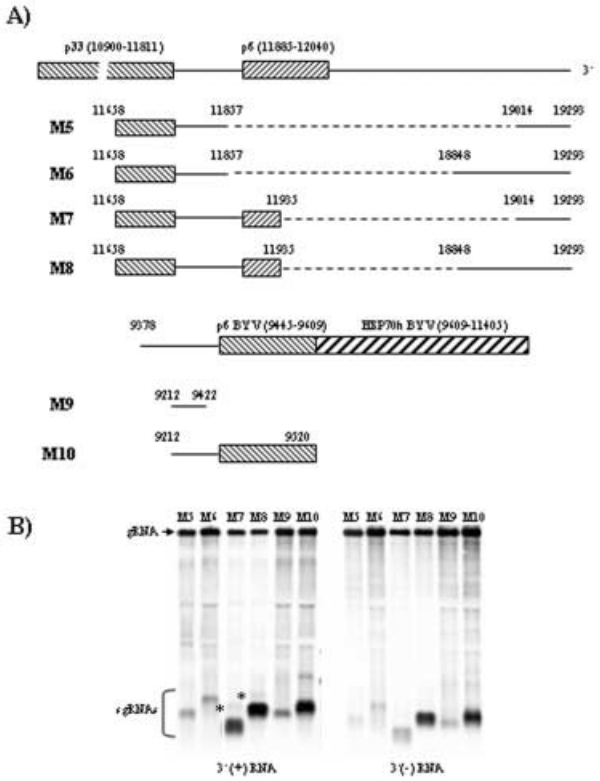

Fig. 2 Location of the p6 sgRNA controller element. (A) Genomic regions of CTV and BYV inserted into a CTV replicon with hatched areas representing ORFs, dashed areas representing deletions and numbers indicating the termini of the inserted fragments. (B) Northern blot hybridization analysis of total RNA isolated from *N. benthamiana* mesophyll protoplasts inoculated with RNA transcripts of mutants M5–M10, and hybridized with 3′ positive- or negative-stranded, RNA-specific riboprobes. The positions of the gRNA and the 3′-terminal sg mRNAs corresponding to p6 and HSP70h genes are indicated. Asterisks mark the p6 sgRNAs.

11885, respectively (Fig. 3A). All of these mutants replicated efficiently and produced positive- and negative-stranded sgRNAs with the exception of mutants M19 and M20 (Fig. 3B). Thus, the 5′ boundary of the HSP70h CE mapped between nucleotides 11858 and 11868.

To identify the minimal region required for production of the HSP70h sgRNA, we examined a series of mutants with both insert borders near the limiting sites (Fig. 3A). Mutant M21, which contained a 58-nt insert, continued to produce the sg mRNA. Mutants M22–M24 had reduced sizes of the insert, and mutant M25 was created by an internal deletion of 26 nt between positions 11858 and 11884. Accumulation of the truncated HSP70h sg mRNA was higher by mutants M21 and M23, less by mutants M22 and M24, and the HSP70h sg mRNA was not produced by mutant M25 (Fig. 3B). These results suggested that the HSP70h CE occurred within a region of approximately 30 nt (nucleotides 11858–11887).

Mapping the p6 CE

Mutant M6 was shown to contain the p6 CE (Fig. 2). To define a minimal region required for production of the p6 sgRNA, we examined a series of mutants containing subsets of sequences within the borders mapped above for the p6 CE. Mutants M26–M30 contained a constant 3′ end at nucleotide 11857 and varying amounts of the 5′ sequences (Fig. 4A). All mutants replicated, but only M6, which contained the region between nucleotides 11658 and 11857, produced the truncated p6 sg mRNA. These results suggested that the 5′-terminus of p6 CE was near position 11658 of the CTV genome. To map the 3′ boundary of the p6 CE, mutants M31, M32 and M33 were constructed with a constant 5′-terminus at position 11658 and variable 3′ ends (Fig. 4A). Mutants M31 and M32 produced the truncated p6 sg mRNA, whereas mutant M33 did not. Mutant M32 accumulated the truncated p6 sg mRNA in much lower amounts than that of M31 (Fig. 4B), suggesting that the p6 CE was located within a region of approximately 109 nt, between positions 11658 and 11766.

Determination of p6 and HSP70h sg mRNAs initiation sites

We previously examined the more abundantly produced sg mRNAs of the six 3′ genes and found that all of them were initiated with an adenylate (Ayllón *et al.*, 2003; Karasev *et al.*, 1997). Their 5′-termini generally corresponded to the base of the predicted 3′-most stem at the edge of the CE, considering positive strand sequence (Ayllón *et al.*, 2004). (It should be borne in mind that it is not known whether the sgRNAs are produced by promotion from the negative-strand sequence or by termination when copying the positive strand.) To examine whether the p6 and HSP70h genes followed a similar pattern, we determined the 5′-termini of their sg mRNAs. The p6 and HSP70h CEs differed dramatically in levels of production of sg mRNAs. The production of sg mRNA by the HSP70h CE appeared to be within the range observed for other CEs examined, e.g. CPm, CP, p18, p13, p20 and p23, when positioned near the 3′-terminus. However, the production of sgRNA by the p6 CE was barely detectable, even when amplified by locating it near the 3′-terminus. Double-stranded (ds) RNA from protoplasts transfected with *in vitro*-produced RNA transcripts of mutant M8 was polyadenylated at the 3′ end, reverse transcribed, and amplified by PCR using oligo dT and a negative-sense CTV specific primer (complementary to nucleotides 18991–19020) to clone the complement of the 5′ end of the HSP70h sg mRNA. All eight resulting clones indicated that the adenylate at position 11884 corresponded to the 5′-terminus (+1 nt) of the HSP70h sgRNA, 1 nt upstream of the p6 start codon and 162 nt upstream of the HSP70h start codon (Fig. 5A). Often the negative strand of dsRNAs has a non-template extra guanylate (Karasev *et al.*, 1997), and four of the eight clones

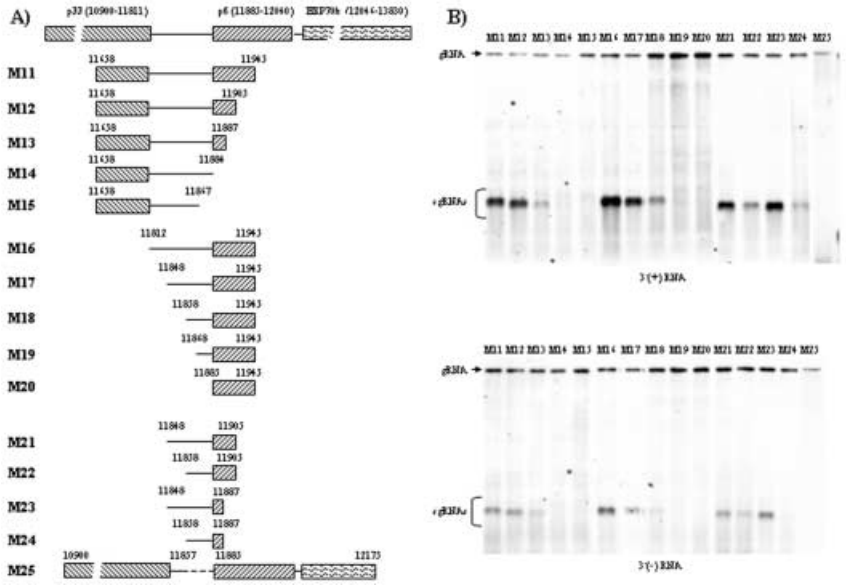

Fig. 3 Determination of 5′ and 3′ boundaries of the HSP70h CE. (A) Representation of the genomic regions ligated into CTV-ΔCla333 to generate mutants M11–M25. The numbers indicate the termini of the inserted fragments. (B) Northern blot hybridization analysis of total RNA isolated from *N. benthamiana* mesophyll protoplasts inoculated with *in vitro*-produced RNA transcripts of mutants M11–M25. The blots were hybridized with positive- or negative-strand-specific riboprobes specific to the 3′-terminus of the genome. The positions of the gRNA and the sg mRNAs are indicated by arrows and brackets, respectively.

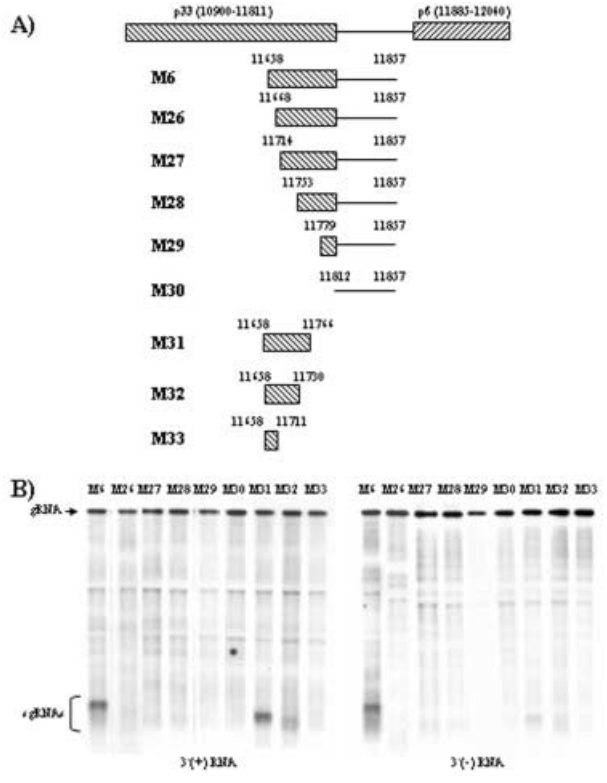

Fig. 4 Delineation of the 5′ and 3′ boundaries of the p6 CE. (A) Genomic regions inserted into the CTV replicon with the genomic sequence indicated above each construct. (B) Northern blot hybridization analysis of RNA isolated from *N. benthamiana* mesophyll protoplasts inoculated with RNA transcripts of mutants M6 and M26–M33. The blots were hybridized with 3′ end positive- or negative-stranded specific RNA probes and the position of gRNA and 3′ sgRNAs are indicated.

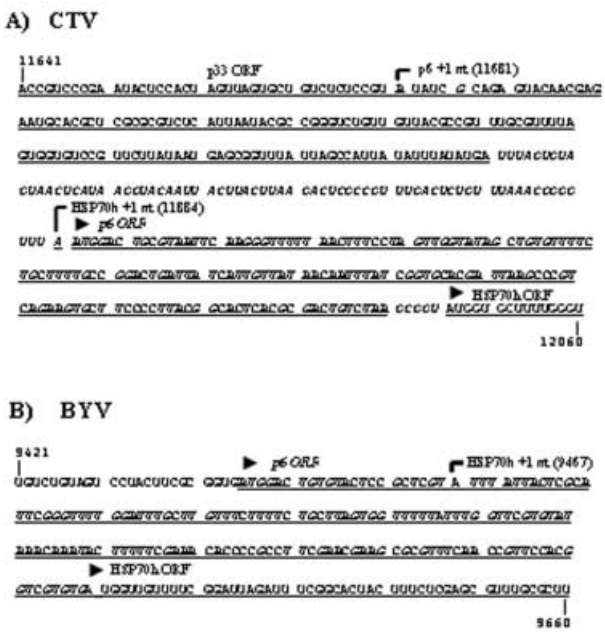

Fig. 5 Determination of the initiation sites (+1) of p6 and HSP70h sg mRNAs. The partial p33 and HSP70h and complete p6 ORFs are underlined. (A) Identification of the +1 nt of the CTV p6 and HSP70h sg mRNAs. The p6 sg mRNA initiation sites are shown in italics and bold. The principal initiation sites are indicated with a curved line. (B) Identification of the BYV HSP70h initiation site when inserted into CTV. The initiation site of the BYV HSP70h sg mRNA produced from mutant M8 is shown by a curved line.

contained the extra guanylate at the 3′-terminus of the negative-stranded HSP70h sgRNA. The position of the +1 nt as the adenylate at nucleotide 11884 was further confirmed by nucleotide sequencing of three clones obtained by RNA ligase-mediated

RACE (RLM-RACE) using as template the positive-stranded HSP70 sgRNA. These results demonstrated that the HSP70h initiation site was located within the HSP70h CE, 26 nt from the 5′ border and 3 nt from the 3′ border of the minimal CE (considering positive strand sequence).

To determine the 5′-terminus of the p6 sgRNA, we also tried to polyadenylate the 3′ end of the dsRNA as described above, but the amount of this sgRNA was too low to map the initiation site. To overcome this problem we used the more abundant positive-stranded p6 sgRNA as source of RNA for RLM-RACE. Nucleotide sequencing of 20 clones obtained showed that 12 initiated with an adenylate at position 11681, 204 nt upstream of the p6 start codon. The remaining eight clones indicated initiation with a guanylate at position 11686 (Fig. 5A). Therefore, p6 CE initiated sgRNA synthesis within the CE at positions −23 and +86 (for adenylate) and −28 and +81 (for guanylate) relative to the fully active element in M31 (described as positive strand sequence).

Examination of the predicted secondary structure of p6 and HSP70h CEs

We compared the sequences and computer-predicted secondary structures (Zuker *et al*., 1999) of the p6 and HSP70h CEs to each other and to other CEs that have been examined. First we compared the conservation of sequence and predicted structure within these areas among different CTV isolates (VT, Mawassi *et al*., 1996; T385, Vives *et al*., 1999; SY568, Yang *et al*., 1999; T30, Albiach-Martí *et al*., 2000; NuagA, Suastika *et al*., 2001) to that of our isolate, T36. The primary sequence of the HSP70h minimal CE was conserved among the different CTV isolates (93% sequence homology with T30, T385 and SY568 and 96% homology with VT and NuagA). However, the p6 CE region between nucleotides 11658 and 11730 was less conserved (80% sequence homology with NuagA and 84% homology with T30, T385, SY568 and VT), but the initiation sites determined (adenylate at position 11681 and guanylate at position 11686) were conserved among all isolates.

The HSP70h CE positive strand sequence was predicted to fold into a long stem-loop of 32 nt with the initiation site at the bottom right-hand side of the stem (Fig. 6A, M8). This predicted structure was conserved among all of the other isolates (data not shown). However, the negative strand was predicted to fold into a small stem-loop of 22 nt that did not contain the +1 nt. Yet this predicted structure was conserved among the other CTV isolates.

The predicted secondary structure of the p6 CE formed two stem-loops, with the +1 site inside the 5′-most stem-loop (Fig. 7A, M6), which was conserved in isolates T30, T385 and SY568, but not in isolates VT and NuagA in which only part of the stem-loop was retained (data not shown). The predicted secondary structures of the negative strand were similar to those of the positive strand and were conserved among the different CTV isolates.

The entire predicted secondary structures of both p6 and HSP70h CEs were conserved when the computer examined the secondary structures of a larger region (300 nt) of plus or minus strand sequences that includes both CEs (data not shown).

To examine possible biological significance of the secondary structures of the p6 and HSP70h CEs, we examined mutants of each CE. The first mutant was designed to disrupt a predicted hydrogen-bonded stem, and the second was designed to restore that structure. Mutant M34 contained four nucleotide changes at positions, with respect to the initiation site, −15 (G to C), −17 (C to G), −19 (C to G), and −20 (A to U) that were predicted to disrupt the predicted secondary structure of HSP70h CE (Fig. 6B). This mutation greatly reduced the production of the sgRNA (Fig. 6D). Compensatory mutations at positions −3 (U to A), −4 (G to C), −6 (G to C) and −8 (C to G) in mutant M35 (Fig. 6C) were predicted to restore the secondary structure, even when folding sequences containing 300 nt. However, these mutations did not restore sgRNA synthesis to wild-type levels (Fig. 6D). These data demonstrate that sequences within this region are important for CE activity. The lack of restoration of sg mRNA synthesis by the predicted compensatory mutations could be due to the importance of primary structure, or the substituted secondary structure might fail to be functional.

To examine the predicted secondary structures of the p6 CE, mutant M36 was constructed by introduction of two nucleotide changes at positions, with respect to the initiation site, −5 (U to A) and −7 (U to A), predicted to disrupt the secondary structure (Fig. 7B). Mutant M37 was constructed with compensatory changes at positions +8 (A to U) and +10 (A to U), predicted to restore the secondary structure (Fig. 7C), even when folding large segments consisting of 300 nt. However, neither of these mutants produced detectable amounts of sg mRNA (Fig. 7D), suggesting that the primary sequence in this area is important for production of the p6 sg mRNA, and providing minimal information about the importance of the predicted secondary structures.

Determination of BYV p6 and HSP70 sg mRNAs initiation sites in a CTV sequence context

We were able to detect the p6 sg mRNA only when amplified by locating its CE near the 3′-terminus of the genome, and even then it was almost undetectable when functioning in a construct also containing the HSP70h CE (Fig. 2B). We next compared its function to that of the analogous p6 CE, that from BYV. We wondered whether a completely different sequence would function as a p6 CE in CTV and, if so, where the sg mRNA would initiate compared with the homologous initiation. We inserted sequences from the CEs of the BYV p6 and HSP70h genes into CTV (Table 1) to create, respectively, mutant M9 (to contain only the p6 CE) and mutant M10 (to contain both p6 and HSP70h CEs) (Fig. 2A). Both mutants replicated and produced sg mRNAs, with the p6 sgRNA produced

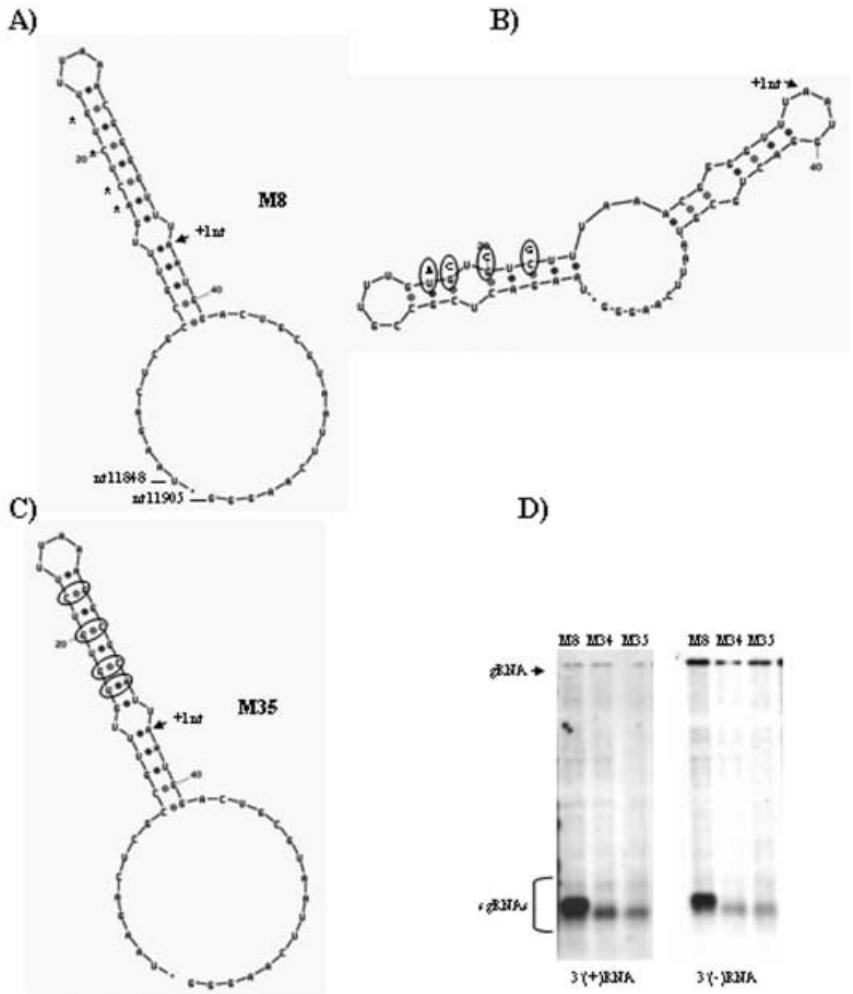

Fig. 6 Secondary structure of HSP70h CEs predicted by the MFOLD program. (A) M8 is the wild-type sequence. The HSP70h sg mRNA initiation site is indicated with an arrow. (B) Mutant M34 with predicted disruption of the base pairing of the upper stem. The mutated nucleotides are shown in circles with wild-type nucleotides shown on top and are indicated in M8 by asterisks. (C) Mutant M35 with compensatory mutations. Nucleotides modified to restore the predicted secondary structure in M35 are circled. (D) Northern blot hybridization analysis of the total RNA isolated from *N. benthamiana* mesophyll protoplasts inoculated with *in vitro*-generated RNA transcripts of these mutants. The blots were hybridized with 3′ RNA probes specific to plus or minus strands, and the gRNA and sgRNA positions are indicated.

in higher amounts from the BYV insert than from the homologous CTV insert (Fig. 2B).

Total RNA extracted from protoplasts infected with mutant M10 was used as template for the polyadenylation of the 3′-terminus of the negative-stranded BYV HSP70h sgRNA. Five clones analysed by sequencing showed that the +1 nt of the BYV HSP70h sg mRNA produced by mutant M10 was the adenylate at position 9467 of the BYV sequence (Fig. 5B), the same as the +1 nt previously mapped for the same sg mRNA within the BYV genome (Peremyslov and Dolja, 2002). All the clones analysed contained an extra guanylate at the 3′ end of the sgRNA negative strand as did the CTV HSP70h sgRNA. The results demonstrate that the CTV replicase complex was able not only to recognize the heterologous CE, but also to initiate sg mRNA synthesis at the same nucleotide as does the BYV replicase complex.

We also tried to map the +1 nt of the BYV p6 truncated sgRNA produced by mutant M9 by polyadenylation of the 3′ end of the sgRNA negative strands. Nucleotide sequencing of eight clones showed a guanylate as the +1 nt, but at three different positions. Two clones initiated at position 9414 (based on the BYV positive-sense sequence), five at position 9418 and one at position 9420 (data not shown). The native +1 nt of the BYV p6 sgRNA within the BYV genome has been mapped to guanylates at three different positions, 9398, 9402 and 9405 (Peremyslov and Dolja, 2002), which are all different from those utilized when inserted into CTV. These data show that initiation of the p6 sgRNA synthesis from the BYV p6 CE within CTV still started with a guanylate, but the positions were not those within its native genome.

DISCUSSION

Because a p6 mRNA had not been detected from CTV-infected cells, there was a question of whether the p6 ORF was translated from a functionally bicistronic message. However, upon amplification by moving the genes near the 3′-terminus, an sg mRNA for each of the p6 and HSP70h genes was found.

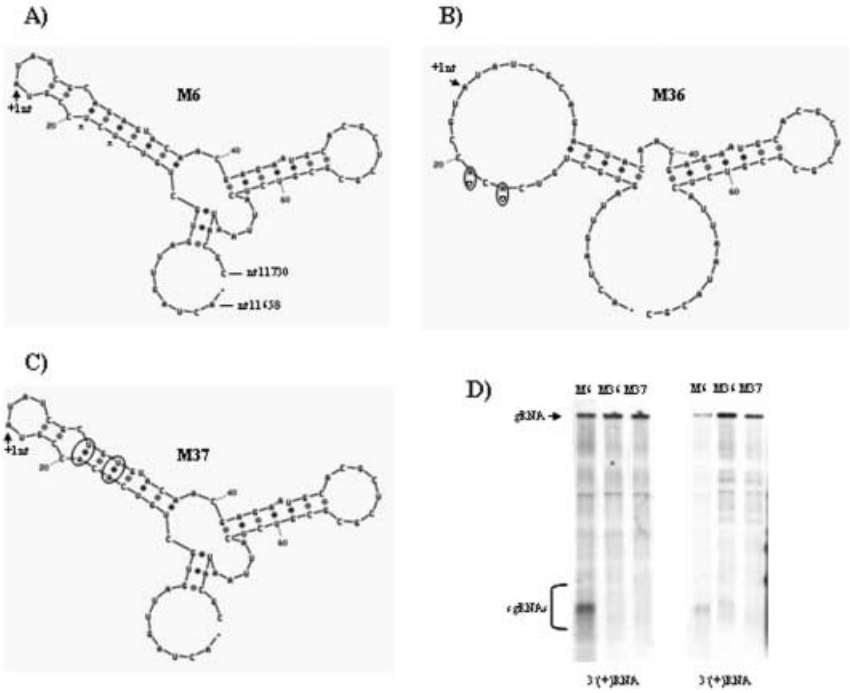

Fig. 7 Predicted secondary structures of p6 CE mutants determined by MFOLD. (A) The wild-type sequence (M6). The +1 nt is indicated with an arrow. (B) Mutant M36 with predicted disruption of the large stem. The mutations of M36 are circled with the wild-type nucleotide shown below the mutated nucleotide and indicated with asterisks in A. (C) Predicted compensatory mutant M37. The mutated nucleotides are circled. (D) Northern blot hybridization analysis of total RNA extracted from *N. benthamiana* mesophyll protoplasts transfected with *in vitro*-produced RNA transcripts of the mutants. The positions of gRNA and sgRNA are indicated by an arrow and a bracket, respectively.

The CEs for both p6 and HSP70h were located further upstream than expected. Other 3′ genes that have been characterized have CEs immediately upstream of their ORFs. Those genes with ORFs preceded by upstream NTRs have higher accumulations of sg mRNAs, and their CEs map within the NTR. The p6 and HSP70h ORFs each have NTRs upstream, 73 and 5 nt, respectively. Thus, the expectation would be that the p6 gene, with a large upstream NTR, would have a CE located within that NTR and be highly expressed, whereas the HSP70h gene would have a CE within the p6 ORF and be expressed at a lower level. However, the opposite result was observed. Yet upon mapping the CEs, the HSP70h CE was positioned upstream of the p6 ORF, mainly within the large NTR between the p33 and p6 ORFs, and the p6 CE is positioned beyond the NTR, within the p33 ORF. Thus, the levels of expression of these genes fit the consensus of higher levels of expression from CEs positioned within NTRs as was observed with the other 3′ genes of CTV.

The HSP70h CE appeared to be similar to other CEs already characterized (Ayllón *et al*., 2004; Gowda *et al*., 2001). The predicted secondary structure contained a stem loop with the initiation site near the base of the stem and the 3′ border of the CE. Like all of the others, the sg mRNA was initiated with an adenylate. An unusual feature was that it was mainly located upstream of the previous ORF within the NTR between the p33 and p6 ORFs, but apparently utilized only about half of that NTR. The generalization has been that sequences within NTRs could be dedicated to the function of CEs. But because only a portion of the NTR was utilized by the HSP70h CE, what would be the function of the rest of this NTR?

The p6 sg RNA was expressed at minimal levels. Even with maximal amplification by moving the CE adjacent to the minimal 3′-NTR required for replication (Satyanarayana *et al*., 1999), the p6 sg mRNA was barely detectable. Interpolation of the native level of p6 sgRNA production by contrasting the difference in production of the p33 or HSP70h mRNAs at their native positions compared with being located near the 3′-terminus leads to the suggestion that only a few molecules of p6 mRNA are produced per cell. It is possible that the unusually long leader of the mRNA also reduces translation. If so, it is not surprising that we were unable to detect p6 in infected cells. In contrast, the BYV p6, even though produced in minimal amounts, appears to be produced in much higher amounts than the CTV p6. Although neither protein is required for replication or assembly of virions, both are required for infection of plants. The BYV p6 has been shown to be necessary for cell-to-cell movement (Alzhanova *et al*., 2000), and to be a transmembrane protein localized to the rough endoplasmic reticulum (Peremyslov *et al*., 2004). Whatever the precise mechanism of the CTV p6 is in movement or infection of plants, it appears to be required in extraordinarily minimal amounts.

The p6 CE appears to function marginally as a *cis*-acting element to interact with the replicase complex to produce an mRNA. In contrast to other CEs, the p6 CE appears to initiate mRNA synthesis at different positions within the CE and within the predicted secondary structures and does not initiate sg mRNA synthesis with a constant nucleotide. This variability in initiation sites was also observed for the BYV p6 mRNA (Peremyslov and Dolja, 2002), but the BYV p6 CE produced more mRNA, even

when inserted into CTV, than did the homologous CTV p6 CE. Yet neither the CTV nor the BYV initiation sites were utilized in the heterologous BYV p6 CE. In addition, the production of the CTV p6 mRNA appeared to be reduced even further by competition with other CEs. More p6 mRNA was produced in the construct with only the p6 CE compared with that with both p6 and HSP70h CEs. Overall, the p6 CE appeared to interact with the replicase complex much less effectively than the other CEs.

In contrast to the other 3′ CEs, the p6 CE has similarities to the 5′ CE located about 600 nt from the 5′-terminus (Ayllón *et al.*, 2004; Gowda *et al.*, 2003). Both initiated sg RNA synthesis with a guanylate (although the p6 CE also initiated with adenylate) and both initiated within the 5′ portion of the CE near the top of a predicted stem loop. However, they differed in that the p6 CE caused the production of a minus-stranded complement of its sgRNA, whereas the 5′ CE did not.

The ten different 3′ CEs of CTV, plus the CEs from BYV that also are able to function in CTV, allow a comparison of a large number of *cis*-acting elements that effectively interact with the viral replicase complex to produce sg mRNAs. The additional observation that there are very large differences in the levels of accumulation of the different mRNAs allows comparisons of strong and weak CEs. Not only do the BYV sequences and structures produce sg mRNAs in CTV, but they can even initiate mRNA synthesis at the native site. Similarly, the coat protein CE of *Beet yellow stunt virus*, another member of the genus *Closterovirus*, was shown to function in BYV (Peremyslov *et al.*, 1999). However, the range of heterologous *cis*-acting elements that function in different closteroviruses is limited. The CEs of LIYV, from the genus *Crinivirus*, did not produce sgRNAs when inserted into CTV (data not presented). Yet so far this approach has provided much less understanding of common properties of CEs than desired. Peremyslov and Dolja (2002) identified 8- and 12-nt sequences upstream of the p6 and HSP70h initiation sites that are common between BYV and CTV. However, when other CEs are examined, these sequences do not appear to be common components of CEs in general. The CTV CEs have predicted stem-and-loop structures, but mutagenesis experiments have not unambiguously demonstrated the need for the secondary structure. Most mutagenesis has resulted in loss of function, suggesting perhaps the need for maintenance of both primary and secondary structures. In addition, the predicted secondary structures for the BYV CEs are not noticeably similar. Yet all of the CTV CEs, except that of p6, have similar predicted stem loops with similarly placed initiation sites. Still, we have no common prediction of a CTV CE. However, even simpler systems that have been extensively examined *in vitro* and *in vivo* have provided definitions of the *cis*-acting elements involved in production of sgRNAs that are difficult to recognize. The *Brome mosaic virus* replicase precisely interacts with sgRNA promoter regions by interacting with four non-contiguous nucleotides and formation of a stem-loop structure, but these four nucleotides can vary in functional heterologous promoters (Sivakumaran *et al.*, 2004). Thus, the CTV replicase complex appears to interact with a precise formula of sequence and structure for producing its mRNAs, but this precise structure is composed of a wide range of different sequences, perhaps forming structural interactions at an order beyond our present recognition. We have found that single nucleotide changes, sometimes even outside the minimal CE but near the initiation site, can prevent, reduce or even increase activity (Ayllón *et al.*, 2003). Quantitative regulation of CTV genes, perhaps, is related to how well the CE conforms to an optimal sequence or configuration. The p6 CE appears to conform just barely.

EXPERIMENTAL PROCEDURES

Construction of mutants

All sequences are presented as positive-stranded RNA. The secondary structures are predicted using the MFOLD program (Zuker *et al.*, 1999). The nucleotide numbering and sequences in this study are according to Satyanarayana *et al.* (2003) (GenBank accession no. AY170468).

Replicon CTV-ΔCla333 has a deletion of nucleotides 10852–18525 from the full-length infectious clone of CTV, pCTV9 (Satyanarayana *et al.*, 1999), retaining both 5′- and 3′-NTRs, ORFs 1a and 1b, plus the 495 3′ nucleotide of the p23 ORF, and has unique restriction sites (*Xho*I, *Pst*I, *Stu*I and *Cla*I) inserted to facilitate insertion of DNA fragments (Gowda *et al.*, 2001). This replicon, which does not produce any 3′ sgRNA, was the basis of all mutants. The description of mutations and the positive (+)- and negative(–)-sense primers used in this study are given in Table 1; nucleotide numbers indicate the termini of the cloned fragments to generate each mutant. All the nucleotide mutations introduced were confirmed by sequencing (Applied Biosystems model 373) at the Interdisciplinary Center for Biotechnology Research DNA sequencing core facility of the University of Florida (Gainesville, FL).

Protoplast transfections and Northern blot hybridization

In vitro capped transcripts were generated from *Not*I-linearized DNA constructs using SP6 RNA polymerase (Epicentre Technologies, WI) (Satyanarayana *et al.*, 1999), and were used directly for polyethylene glycol-mediated transfection of mesophyll protoplasts from *N. benthamiana* ($\sim 1 \times 10^6$) (Navas-Castillo *et al.*, 1997). Protoplasts were harvested at 4 dpi, and total RNA was extracted (Navas-Castillo *et al.*, 1997) and analysed by Northern blot hybridization using positive- and negative-stranded RNA-specific riboprobes corresponding to the 3′-terminus of the genome (Satyanarayana *et al.*, 1999). The riboprobes were examined by their specificity and equalized using double-stranded RNAs.

Mapping of initiation site of CTV and BYV HSP70h sg mRNAs

Total RNA, containing CTV-specific single- and double-stranded RNAs, extracted from protoplasts infected with *in vitro* RNA transcripts of mutant M8 (CTV HSP70h) or mutant M10 (BYV HSP70h) was used as template to determine the 5′-termini of HSP70h sgRNA. Total RNA was denatured at 90 °C, 3′-polyadenylated by yeast poly(A) polymerase (US Biochemicals), and reverse transcribed using AMV (US Biochemicals) and oligo(dT) (M111: 5′-GGTCTCGAG$(T)_{18}$-3′). The 5′-termini of the HSP70h sg mRNAs was amplified with M111 and the negative-sense primer C156 (complementary to nucleotides 19020–18991). The amplified products were ligated into pGEM®-T Easy according to the manufacturer's instructions (Promega). The resulting clones were sequenced as described above.

Mapping of initiation site of CTV p6 sgRNA

The 5′-terminus of p6 sgRNA was determined using the FirstChoice 5′ RLM-RACE kit according to the manufacturer's instructions (Ambion). Total RNA extracted from protoplasts inoculated with mutant M6 was treated with calf intestinal phosphatase and tobacco acid pyrophosphatase, followed by ligation of the 5′ RACE adapter to the 5′-termini of the decapped mRNAs. Reverse transcription was performed using the random primers provided with the kit, followed by PCR amplification with the 5′ RACE positive sense outer primer and the negative sense primer C1466 complementary to nucleotides 19061–19038. Subsequently, sufficient amounts of DNA were amplified using as template the previously amplified product and the 5′ RACE positive-sense inner primer and the negative-sense primer C1467 complementary to nucleotides 18961–18983. The final PCR product was cloned into pGEM-T Easy (Promega), and several clones were sequenced.

ACKNOWLEDGEMENTS

We thank John Cook, Cecile Robertson and Judy Harber for technical assistance, and Dr Jaime Cubero and John Cook for critically reading the manuscript. This research was supported by the Florida Agricultural Experiment Station, an endowment from the J. R. and Addie Graves family, and grants from the Florida Citrus Production Research Advisory Council, US-Israel BARD, and USDA/ARS cooperative agreement 58-6617-4-018, and was approved for publication as University of Florida Agricultural Experiment Station Journal Series No. R-10535. M.A.A. was the recipient of a postdoctoral fellowship from the Ministerio de Educación y Ciencia (Spain).

REFERENCES

Albiach-Martí, M.R., Mawassi, M., Gowda, S., Satyanarayana, T., Hilf, M.E., Shanker, S., Almira, E.C., Vives, M.C., López, C., Guerri, J., Flores, R., Moreno, P., Garnsey, S.M. and Dawson, W.O. (2000) Sequences of Citrus tristeza virus separated in time and space are essentially identical. *J. Virol.* **74**, 15–23.

Alzhanova, D.V., Hagiwara, Y., Peremyslov, V.V. and Dolja, V.V. (2000) Genetic analysis of the cell-to-cell movement of beet yellows closterovirus. *Virology*, **267**, 192–200.

Ayllón, M.A., Gowda, S., Satyanarayana, T. and Dawson, W.O. (2004) *cis*-acting elements at opposite ends of the *Citrus tristeza virus* genome differ in initiation and termination of subgenomic RNAs. *Virology*, **322**, 41–50.

Ayllón, M.A., Gowda, S., Satyanarayana, T., Karasev, A.V., Adkins, S., Mawassi, M., Guerri, J., Moreno, P. and Dawson, W.O. (2003) Effects of modification of the transcription initiation site context on *Citrus tristeza virus* subgenomic RNA synthesis. *J. Virol.* **77**, 9232–9243.

Gowda, S., Ayllón, M.A., Satyanarayana, T., Bar-Joseph, M. and Dawson, W.O. (2003) Transcription strategy in a closterovirus: a novel 5′-proximal controller element of citrus tristeza virus produces 5′- and 3′-terminal subgenomic RNAs and differs from 3′ open reading frame controller elements. *J. Virol.* **77**, 340–352.

Gowda, S., Satyanarayana, T., Ayllón, M.A., Albiach-Martí, M.R., Mawassi, M., Rabindran, S., Garnsey, S.M. and Dawson, W.O. (2001) Characterization of the *cis*-acting elements controlling subgenomic mRNAs of *Citrus tristeza virus*: production of positive- and negative-stranded 3′-terminal and positive-stranded 5′-terminal RNAs. *Virology*, **286**, 134–151.

Hilf, M.E., Karasev, A.V., Pappu, H.R., Gumpf, D.J., Niblett, C.L. and Garnsey, S.M. (1995) Characterization of citrus tristeza virus subgenomic RNAs in infected tissue. *Virology*, **208**, 576–582.

Karasev, A.V., Boyko, V.P., Gowda, S., Nikolaeva, O.V., Hilf, M.E., Koonin, E.V., Niblett, C.L., Cline, K., Gumpf, D.J., Lee, R.F., Garnsey, S.M., Lewandowski, D.J. and Dawson, W.O. (1995) Complete sequence of the citrus tristeza virus RNA genome. *Virology*, **208**, 511–520.

Karasev, A.V., Hilf, M.E., Garnsey, S.M. and Dawson, W.O. (1997) Transcriptional strategy of closteroviruses: mapping the 5′-termini of the citrus tristeza subgenomic RNAs. *J. Virol.* **71**, 6233–6236.

Karasev, A.V., Nikolaeva, O.V., Koonin, E.V., Gumpf, D.J. and Garnsey, S.M. (1994) Screening of the closterovirus genome by degenerate primer-mediated polymerase chain reaction. *J. Gen. Virol.* **75**, 1415–1422.

van Marle, G., Dobbe, J.C., Gultyaev, A.P., Luytjes, W., Spaan, W.J.M. and Snijder, E.J. (1999) Arteriovirus discontinuous mRNA transcription is guided by base pairing between sense and antisense transcription-regulating sequences. *Proc. Natl Acad. Sci. USA*, **96**, 12056–12061.

Mawassi, M., Mietkiewska, E., Gofman, R., Yang, G. and Bar-Joseph, M. (1996) Unusual sequence relationship between two isolates of citrus tristeza virus. *J. Gen. Virol.* **77**, 2359–2364.

Miller, W.A. and Koev, G. (2000) Synthesis of subgenomic RNAs by positive-strand RNA viruses. *Virology*, **273**, 1–8.

Navas-Castillo, J., Albiach-Martí, M.R., Gowda, S., Hilf, M.E., Garnsey, S.M. and Dawson, W.O. (1997) Kinetics of accumulation of citrus tristeza virus RNAs. *Virology*, **228**, 92–97.

Pappu, H.R., Karasev, A.V., Anderson, E.J., Pappu, S.S., Hilf, M.E., Febres, V.J., Eckloff, R.M.G., McCaffery, M., Boyko, V., Gowda, S., Dolja, V.V., Koonin, E.V., Gumpf, D.J., Cline, K.C., Garnsey, S.M., Dawson, W.O., Lee, R.F. and Niblett, C.L. (1994) Nucleotide sequence and organization of eight-3′ open reading frames of the citrus tristeza closterovirus genome. *Virology*, **199**, 35–46.

Peremyslov, V.V. and Dolja, V.V. (2002) Identification of the subgenomic mRNAs that encode 6-kDa movement protein and Hsp70 homolog of *Beet yellows virus*. *Virology*, **295**, 299–306.

Peremyslov, V.V., Hagiwara, Y. and Dolja, V.V. (1999) HSP70 homolog functions in cell-to-cell movement of a plant virus. *Proc. Natl Acad. Sci. USA*, **96**, 14771–14776.

Peremyslov, V.V., Pan, Y.W. and Dolja, V.V. (2004) Movement protein of a closterovirus is a type III integral transmembrane protein localize to the endoplasmic reticulum. *J. Virol.* **78**, 3704–3709.

Satyanarayana, T., Gowda, S., Ayllón, M.A., Albiach-Martí, M.R. and Dawson, W.O. (2002a) Mutational analysis of the replication signals in the 3-nontranslated region of *Citrus tristeza virus*. *Virology*, **300**, 140–152.

Satyanarayana, T., Gowda, S., Ayllón, M.A., Albiach-Martí, M.R., Rabindran, S. and Dawson, W.O. (2002b) The p23 protein of Citrus tristeza virus controls asymmetrical RNA accumulation. *J. Virol.* **76**, 473–483.

Satyanarayana, T., Gowda, S., Ayllón, M.A. and Dawson, W.O. (2003) Frameshift mutations in infectious cDNA clones of *Citrus tristeza virus*: a strategy to minimize toxicity of viral sequences to *Escherichia coli*. *Virology*, **313**, 481–491.

Satyanarayana, T., Gowda, S., Boyko, V.P., Albiach-Martí, M.R., Mawassi, M., Navas- Castillo, J., Karasev, A.V., Dolja, V., Hilf, M.E., Lewandowski, D.J., Moreno, P., Bar-Joseph, M., Garnsey, S.M. and Dawson, W.O. (1999) An engineered closterovirus RNA replicon and analysis of heterologous terminal sequences for replication. *Proc. Natl Acad. Sci. USA*, **96**, 7433–7438.

Sawicki, S.G. and Sawicki, D.L. (1998) A new model for coronavirus transcription. *Adv. Exp. Med. Biol.* **440**, 215–219.

Sivakumaran, K., Choi, S.-K., Hema, M. and Kao, C.C. (2004) Requirement for *Brome mosaic virus* subgenomic RNA synthesis *in vivo* and replicase–core promoter interactions *in vitro*. *J. Virol.* **78**, 6091–6101.

Suastika, G., Natsuaki, T., Terui, H., Kano, T., Ieki, H. and Okuda, S. (2001) Nucleotide sequence of *Citrus tristeza virus* seedling yellows isolate. *J. Gen. Plant Pathol.* **67**, 73–77.

Vives, M.C., Rubio, L., López, C., Navas-Castillo, J., Albiach-Martí, M.R., Dawson, W.O., Guerri, J., Flores, R. and Moreno, P. (1999) The complete genome sequence of the major component of a mild citrus tristeza virus isolate. *J. Gen. Virol.* **80**, 811–816.

White, K.A. (2002) The premature termination model: a possible third mechanism for subgenomic mRNA transcription in (+)-strand RNA viruses. *Virology*, **304**, 147–154.

Yang, Z.N., Mathews, D.M., Dodds, J.A. and Mirkov, T.E. (1999) Molecular characterization of an isolate of citrus tristeza virus that causes severe symptoms in sweet orange. *Virus Genes*, **19**, 131–142.

Zuker, M., Mathews, D.H. and Turner, D.H. (1999) Algorithms and thermodynamics for RNA secondary structure prediction. A practical guide. In *RNA Biochemistry and Bio/Technology* (Barciszewski, J. and Clark, B.F.C., eds). Dordrecht/Norwell, MA: Kluwer Academic Publishers, pp. 11–43.